

LASER APPLICATIONS AND OTHER TOPICS OF QUANTUM ELECTRONICS

PACS numbers: 41.75.Fr; 42.60.Jf; 42.65.Ky; 42.65.Re; 42.70.Mp
DOI: 10.1070/QE2014v044n01ABEH015224

Scanning cross-correlator for monitoring uniform 3D ellipsoidal laser beams

V.V. Zelenogorskii, A.V. Andrianov, E.I. Gacheva, G.V. Gelikonov, M. Krasilnikov, M.A. Mart'yanov, S.Yu. Mironov, A.K. Potemkin, E.M. Syresin, F. Stephan, E.A. Khazanov

Abstract. **The specific features of experimental implementation of a cross-correlator with a scan rate above 1600 cm s^{-1} and a spatial delay amplitude of more than 15 mm are considered. The possibility of measuring the width of femtosecond pulses propagating in a train 300 μs in duration with a repetition rate of 1 MHz is demonstrated. A time resolution of 300 fs for the maximum time window of 50 ps is attained. The cross-correlator is aimed at testing 3D pulses of a laser driver of an electron photo-injector.**

Keywords: *cross-correlator, pulse temporal profile.*

1. Introduction

The electron beams used in modern free-electron lasers (FELs) should satisfy very stringent requirements. A high peak current (on the order of 1 kA after several stages of electron bunch compression), a low normalised transverse emittance (less than 1 mm mrad), and a small energy spread (~0.1%) are necessary for efficient operation of such systems as the FEL in Hamburg (FLASH, DESY, Germany); the American project LCLS (Linac Coherent Light Source) based on the Standford Linear Accelerator (SLAC); and the European X-ray FEL (European XFEL, Germany), which is being developed in Hamburg.

Currently, the most promising electron beam sources are injectors based on the use of high-frequency guns with a photocathode, emitting electrons under irradiation by the so-called cathode laser. In recent years, these injectors have provided beams with parameters necessary for successful FEL operation (peak current ~ 50 A, electron beam duration 10–20 ps, and normalised emittance below 1 mm mrad). A distinctive feature of the FELs based on superconducting linear accelerators (FLASH, European XFEL) is a high on–off time ratio of cathode-laser pulses. The electron beams in these accelerators are modulated in time as follows. Short bunches with a width of several picoseconds are combined into relatively long (from 1 μs to 10 ms) trains, propagating with a repetition rate of 1–50 Hz [1–4]. Under these conditions, the average FEL radiation power increases, due to which many research problems can be solved. A high peak power is obtained by providing necessary individual parameters of each bunch in the train. In particular, to obtain a beam with desired brightness, one needs electron bunches with a transverse normalised emittance of ~1 mm mrad (or even less) and a charge no less than 1 nC. Moreover, these parameters must be reproduced with a high stability both within a train and from train to train.

Generation of low-emittance electron beams in high-frequency photoguns is a complex multiparameter problem. Since a significant fraction of uncorrelated emittance is formed during photoemission, the shape of the cathode-laser pulse plays an important role in optimisation of electron beam parameters. Therefore, profiling of the temporal shape of a cathode-laser pulse is a very important problem. A transition from Gaussian to rectangular shape changes to a great extent the space charge structure in the electron bunch emitted by the photocathode.

Currently, studies aimed at generating such beams are under way in many laboratories. Photo-injectors with laser drivers are used in most cases. For example, electron bunches with a charge of 1 nC and an emittance of 2.1 mm mrad at an electron energy of 100 MeV have been obtained on the FLASH photo-injector of the DESY accelerator for 10-ps Gaussian laser pulses. The DESY-PITZ photo-injector provided an emittance of ~0.7 mm mrad for trapezoidal laser pulses with a width of 21.5 ps and a leading-edge width of 2 ps [2].

The electron bunch emittance can be reduced even more using 3D profiling. In this case, a distribution in the form of a 3D ellipsoid (with a time coordinate and two transverse spatial coordinates) with a uniform electron density corresponds to the strictly linear radial dependence of the forces of electron-bunch space charge (Kapchinsky–Vladimirsky distribution [5]). Under these conditions, the transverse emittance is minimally increased. The generation of ellipsoidal pulses by a cathode laser is considered to be the first step in this direction. The requirements for the electron bunch parameters impose the corresponding requirements on the parameters of laser pulses. The spatial and temporal lasing characteristics should correspond to the analogous parameters of the electron beam. Below we will refer to picosecond pulses and long trains of micropulses as micropulses and macropulses, respectively. The energy of micropulses that is necessary to form electron bunches depends on the photocathode efficiency and the total bunch charge. The most stable and efficient Cs_2Te cathodes, which can operate for many months with an efficiency of

V.V. Zelenogorskii, A.V. Andrianov, E.I. Gacheva, G.V. Gelikonov, S.Yu. Mironov, A.K. Potemkin, E.A. Khazanov Institute of Applied Physics, Russian Academy of Sciences, ul. Ul'yanova 46, 603950 Nizhnii Novgorod, Russia; e-mail: vvmailv@mail.ru;
M. Krasilnikov, F. Stephan Photo Injector Test Facility DESY-PITZ, 15738, Germany, Zeuthen, Platanenalle, 6;
M.A. Mart'yanov European Organization for Nuclear Research CERN, 1211 Switzerland, Geneva, CH 23;
E.M. Syresin Joint Institute for Nuclear Research, ul. Joliot-Curie 6, 141980 Dubna, Moscow region, Russia

Received 11 May 2013; revision received 16 July 2013
Kvantovaya Elektronika **44** (1) 76–82 (2014)
Translated by Yu.P. Sin'kov

~5% call for a lasing wavelength of 0.2–0.3 μm and micropulse energy ~1–10 μJ.

The aforementioned requirements to the lasing parameters should be supplemented with the requirements for high stability of micropulse repetition frequency and tuning this frequency to the high pump frequency of accelerator modules. Commercial lasers cannot satisfy all these requirements.

Currently, we are developing a laser driver for the linear electron accelerator DESY. The output laser radiation at a wavelength of 262 μm is expected to have a form of a set of 3D micropulses of ellipsoidal shape with an energy up to 15 μJ, width of 6–7 ps, and a repetition frequency of 1 MHz. The micropulses are combined into 300-μs macropulses, which are repeated with a frequency of 1–10 Hz.

When developing and exploiting cathode lasers with ellipsoidal micropulses (3D pulses), one must perform spatial and temporal measurements of the radiation intensity. It is most convenient to do using a cross-correlator. To this end, a cathode laser, along with the operating channel, which emits picosecond (main) pulses, should be equipped with a diagnostic channel, emitting pulses much shorter than the operating channel pulses and with a minimally possible time jitter with respect to the operating channel pulses. For a laser driver with 3D ellipsoidal pulses, a cross-correlator is a key unit both in the formation of 3D ellipsoidal light structure and during laser operation.

As will be shown below, the scan rate of the diagnostic channel in lasers of this type is rather high. This problem is difficult to solve using conventional time scanning methods. In this study we propose a design of a cross-correlator that successfully solves the problem of monitoring 3D ellipsoidal pulses from a cathode laser.

2. Specificity of scanning the cross-correlator for a laser driver of an electron accelerator

As was noted above, the fundamental difference between the cross-correlator scheme for measuring cathode-laser pulses and the conventional schemes is the high scan rate. Let us estimate it.

Figure 1 presents a time diagram explaining the scanning of micropulses in the cross-correlator. It can be seen that, in the time interval of the macropulse (T = 300 μs), one must scan the operating channel pulse with a width t_m by a short diagnostic-channel pulse with a width t_d. To ensure confident diagnostics of micropulses, the scan window width t_w should exceed t_m. The maximum number of 'scans' that can be done during the time T does not exceed the number of pulses N per train (macropulse). Each subsequent 'scans' is shifted with respect to the previous one by a time interval $\Delta t_p = t_m/N$. For a scan window with a width t_w = 15 ps and N = 300, $\Delta\tau$ = 50 fs. This number gives the limiting time resolution of the cross-correlator when an infinitely short pulse is used in the diagnostic channel.

To make the diagnostic channel pulse shift by a value t_w during time T, the rate of change in its spatial delay with respect to the operating channel pulse in the case of propagation of these pulses in air, $V = ct_w/T$, should be 1500 cm s^{-1} (c is the speed of light) and remain constant during the entire scanning interval t_w. The real width of diagnostic channel pulses in the cross-correlator under consideration is larger than that presented in Fig. 1 by a factor of 6 and amounts to 300 fs (see below); correspondingly, the time resolution will be lower by a factor of 5, but the scan rate should remain, as previously, no less than 1500 cm s^{-1}.

3. Physical model of second-harmonic generation in a cross-correlator

The correlator operation is based on a nonlinear optical process: generation of the sum frequency. Our device generates the second harmonic because the operating and diagnostic pulses have identical frequencies. The correlator scheme (Fig. 2) implements noncollinear interaction between the main (1) and diagnostic (2) pulses, at which sum-frequency pulses (3) are generated. The dependence of the energy of the sum-frequency signal W_3 on the time delay τ of the diagnostic pulse with respect to the main pulse is (under certain conditions) a cross-correlation function (CCF) of the intensity profiles of the interacting pulses.

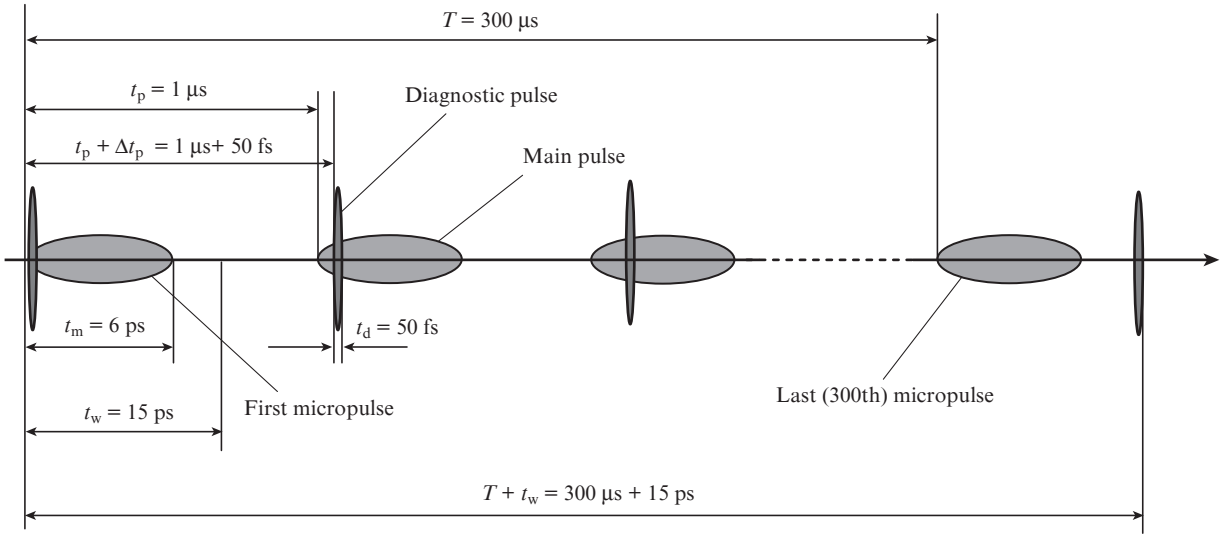

Figure 1. Time diagram of 3D pulsed diagnostics.

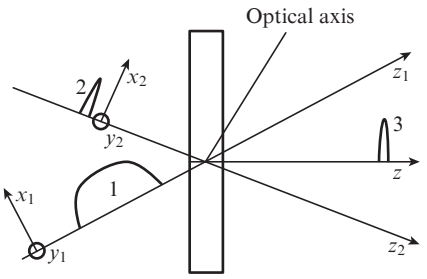

Figure 2. Interaction of pulses in a nonlinear crystal.

The main cross-correlator elements are a nonlinear crystal, in which the frequencies of the operating- and diagnostic-channel pulses are summed, and the delay line in the diagnostic channel. The requirements to the delay line will be formulated below. Now, we will determine the optimal conditions for sum-frequency generation and present the results of 3D numerical simulation as applied to the experimentally realized parameters. This must be done to provide adequate representation of the real parameters of operating-channel radiation in terms of CCF.

The nonlinear noncollinear process of sum-frequency generation (oo–e phase matching) is described by a system of truncated quasi-optical equations:

$$\hat{L}_1 A_1 = -\mathrm{i}\left[\frac{2\pi\chi^{(2)}\omega_1^2}{k_1 c^2 \cos(\alpha/2)}\right] A_2 A_3^* \exp\{-\mathrm{i}[k_3 - 2k_1\cos(\alpha/2)]z\},$$

$$\hat{L}_2 A_2 = -\mathrm{i}\left[\frac{2\pi\chi^{(2)}\omega_2^2}{k_2 c^2 \cos(\alpha/2)}\right] A_1 A_3^* \exp\{-\mathrm{i}[k_3 - 2k_1\cos(\alpha/2)]z\}, \quad (1)$$

$$\hat{L}_3 A_3 = -\mathrm{i}\left[\frac{2\pi\chi^{(2)}\omega_3^2}{k_3 c^2}\right] A_1 A_2^* \exp\{\mathrm{i}[k_3 - 2k_1\cos(\alpha/2)]z\}.$$

Here, A_n are the complex amplitudes of strengths ($n = 1, 2, 3$); α is the angle between the propagation directions of the diagnostic and main pulses in the nonlinear crystal;

$$\hat{L}_n = \frac{\partial}{\partial z} + \frac{1}{u_n}\frac{\partial}{\partial t} + \frac{\mathrm{i}}{2k_n}\Delta_\perp - \frac{\mathrm{i}k_{2n}}{2}\frac{\partial^2}{\partial t^2} + \rho_n\frac{\partial}{\partial x}$$

is a linear differential operator; ω_n and k_n are the central frequencies and wave numbers, respectively; u_n are the components of the group velocities in the z axis; $\rho_1 = \alpha/2$ and $\rho_2 = -\alpha/2$ are the angles under which pulses 1 and 2 propagate; $\rho_3 = \rho_{\text{walk-off}}$ is the walk-off angle of the extraordinary wave; k_{2n} are the parameters characterising the group-velocity dispersion of the interacting pulses; and $\chi^{(2)}$ is the quadratic susceptibility of the medium.

The nonlinear process must be implemented in the unsaturated regime, i.e., the energy of the sum-frequency radiation W_3 at the output of the nonlinear crystal should satisfy the condition $W_3 \ll W_1, W_2$, where W_1 and W_2 are the energies of the main and diagnostic pulses, respectively. It is important to reduce the influence of the dispersion effects: group walk-off and group-velocity dispersion of pulses, as well as the diaphragm-aperture effect, caused by the angular walk-off of the extraordinary wave.

Another important aspect is the accuracy of adjusting the phase matching angle θ_s. The optimal adjustment is obtained when the following condition is satisfied:

$$\Delta kL/2 = [k_3 - 2k_1\cos(\alpha/2)]L/2 \ll 1. \quad (2)$$

Here, L is the nonlinear-crystal thickness. When the aforementioned requirements are satisfied, the measured dependence of the sum-frequency radiation energy on the time delay is proportional to the CCF of the intensities I_1 and I_2 of the main and diagnostic pulses:

$$W_3(\tau) \propto \int_{-\infty}^{+\infty} I_1(t-\tau) I_2(t)\,\mathrm{d}t. \quad (3)$$

If the diagnostic pulse is a δ-function in time, the measured dependence of the sum-frequency energy is proportional to the main-pulse intensity. In this context, the case where the diagnostic pulse is much shorter than the main pulse (i.e., $t_\mathrm{d} \ll t_\mathrm{m}$) is implemented in the correlator under consideration.

Generally, when the phase-matching conditions are violated and the thickness of nonlinear crystal is incorrectly chosen, the measured dependence $W_3(\tau)$ is not a CCF, and this circumstance significantly hinders the determination of the main-pulse temporal structure.

The initial conditions for the main and diagnostic 3D ellipsoidal pulses will be set using the following model pulses:

$$A_1 = A_{10}\cos^2\left(\frac{\pi}{2}P_1^4\right)\exp(\mathrm{i}\alpha t_1^2/2),$$

$$P_1 = \left(\frac{2x_1}{D_1}\right)^2 + \left(\frac{2y_1}{D_1}\right)^2 + \left(\frac{2t_1}{T_1}\right)^2,\ A_1(P_1 > 1) = 0, \quad (4)$$

$$A_2 = A_{20}\exp\left[-2\ln 2\left(\frac{x_2^2}{D_2^2} + \frac{y_2^2}{D_2^2} + \frac{t_2^2}{T_2^2}\right)\right].$$

Here, T_1 and T_2 are the widths of pulses 1 and 2, respectively, and D_1 and D_2 are the diameters of the corresponding beams. Note that the expression for field A_1 takes into account the quadratic dependence of the phase on time, i.e., the linear frequency chirp. As will be shown below, this consideration must be performed to adequately describe the operation of the laser driver cross-correlator.

To solve Eqn (1) with initial conditions (4), we developed a numerical code to simulate the cross-correlator operation. Typical values of the parameters of cathode-laser micropulses were used: energies $W_1 = 0.1$ μJ and $W_2 = 0.2$ μJ, beam diameters $D_1 = D_2 = 0.5$ mm, and pulse widths $T_1 = 7$ ps and $T_2 = 0.2$ ps. The centre wavelengths of the main and diagnostic signals are identical: 1.03 μm. In accordance with these parameters and with allowance for the results of numerical simulation, we chose a 1-mm-thick BBO crystal as a nonlinear crystal for our cross-correlator. The crystal was cut in the direction of the first-type (oo–e) phase matching at the angles $\vartheta = 23.4°$ and $\varphi = 30°$ to the optical axis. The dependence of the conversion efficiency on the phase-matching angle detuning is close to the corresponding dependence for plane waves. The total phase-matching width in the critical plane for this crystal was 12 mrad at an internal convergence angle of 3° for the diagnostic and operating beams.

At a small detuning from the phase-matching angle (within the experimental error), the correlator is expected to adequately reproduce both the time CCF and the transverse

distribution of pulse intensity at different instants (3D pulse structure). Figure 3 shows the results of simulating the time profile of the radiation tested and the CCF under conditions of exact phase matching and detunings by 2.5 and 5 mrad from the phase-matching angle. It can be seen that the CCF shape and intensity distribution for the second-harmonic radiation change only slightly at deviations of the nonlinear crystal from the exact phase-matching direction within ±2.5 mrad. For these detunings, the correlation coefficient between the CCF and time intensity distribution exceeds 0.97.

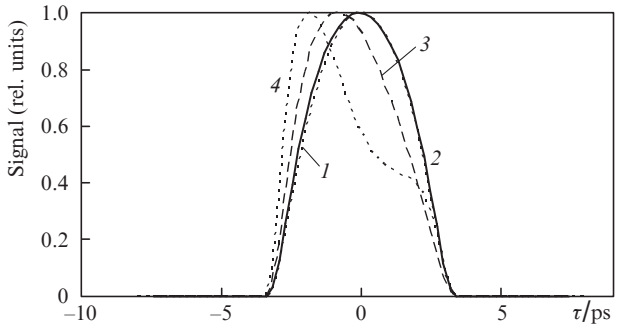

Figure 3. Time intensity profiles of (*1*) a tested signal and (*2*)–(*4*) a cross-correlator signal at exact phase matching (*2*) and at detunings from the phase-matching angle by (*3*) 2.5 and (*4*) 5 mrad.

If there is a detuning of the phase-matching angle, the transverse intensity distribution of the 3D pulse is also distorted. Figure 4 shows intensity distribution patterns in the plane of the central (i.e., at $\tau = 0$) cross section of the 3D pulse at the fundamental frequency and at the second-harmonic frequency for different detunings from the phase-matching angle. The correlation coefficient between the spatial intensity

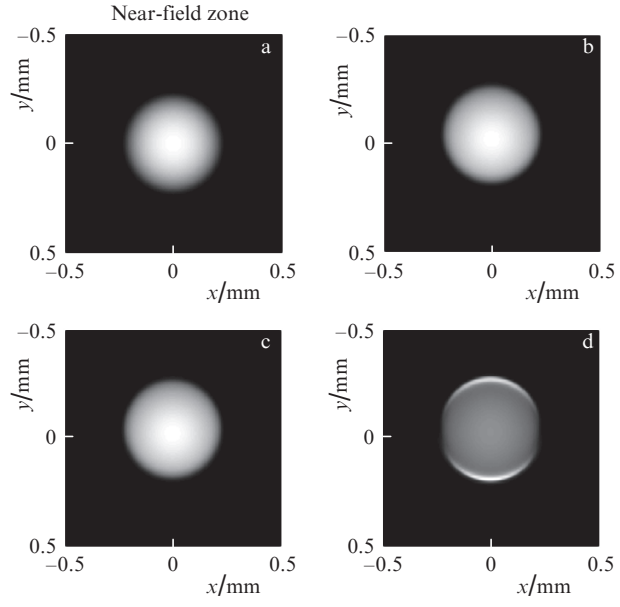

Figure 4. 3D-pulse intensity distributions in the central cross section for the (a) fundamental harmonic and (b–d) the second harmonic in a crystal oriented exactly at the phase-matching angle and detuned from the phase-matching angle by (c) 2.5 and (d) 5 mrad.

distribution at the fundamental frequency (Fig. 4a) and the intensity distribution at the second-harmonic frequency at exact phase matching and at detunings from the phase-matching angle by 2.5 and 5 mrad are, respectively, 0.947, 0.945 and 0.844. Hence, one can draw the following conclusion: at deviations of a nonlinear crystal from the exact phase-matching direction within ±2.5 mrad the shape of the cross-correlator pulse repeats that of the operating-channel pulse. This accuracy of crystal setting can easily be implemented in experiments.

4. Design of the scanning delay line

As was shown in Section 2, our laser driver calls for a delay line shifting the diagnostic pulse with respect to the operating pulse over a distance of 4.5 mm at a constant velocity of 1500 cm s^{-1}. Standard solutions to this problem in the form of a 'trombone' with two mirrors, oriented at an angle of 45° with respect to the optical axis and mounted on the solenoid core, do not provide the desired parameters. In addition, when scanning is performed, the radiation wave vector should not deviate (in order to retain the conditions of second-harmonic generation in the cross-correlator). Will and Klemz [6] reported a design of a cross-correlator with a scanning delay line, in which the scanning mirror moves uniformly with a velocity of 30 cm s^{-1}. Since this mirror is located in a regenerative 23-pass amplifier, the effective velocity is 690 cm s^{-1}, which is close to the desired value, but, nevertheless, is still insufficient.

A delay line made of a single-mode polarisation-maintaining optical fibre was used as cross-correlator scanner. This fibre (80 m long) was coiled as a spiral onto a thin piezoelectric ceramic washer [7]. When a linearly increasing sawtooth voltage (0–400 V) is applied to the washer electrodes, the fibre length linearly increases, due to which scanning can be performed within the scan window for 300 μs with a limiting constant rate of more than 1500 cm s^{-1}.

A high-speed video camera, which is intended to record the transverse intensity distribution of 3D pulses, must be fast enough to capture all frames for 300 μs; to this end, the rate must be no less than 3300 frames s^{-1} [8]. In the experiments described below, we used a photodiode and a standard CCD camera.

5. Experiment

In accordance with the theory [9], for the second-harmonic intensity to be proportional to the operating-channel radiation intensity, the frequency doubling efficiency η should be much smaller than unity. We implemented the relation $\eta <$ 0.1% in our experiment.

As was mentioned above, the laser driver has two channels: a main channel for irradiating the cathode of the electron photo-injector and a diagnostic channel for the cross-correlator. Both channels are formed by the same radiation source: a pulsed fibre laser. The mean power at the output of fibre amplifiers in each channel is 0.5–1 W. The pulse width (FWHM) is 100 ps. The emission spectrum with a centre wavelength $\lambda_0 \approx 1.03$ μm in both channels has a width $\Delta\lambda =$ 11 nm (FWHM) (Fig. 5). Compressors based on diffraction gratings are mounted at the output of each channel. Figure 5 shows the autocorrelation function (ACF) of the operating-channel pulse and the emission spectra of the diagnostic and operating channels when the optical compressor is tuned to

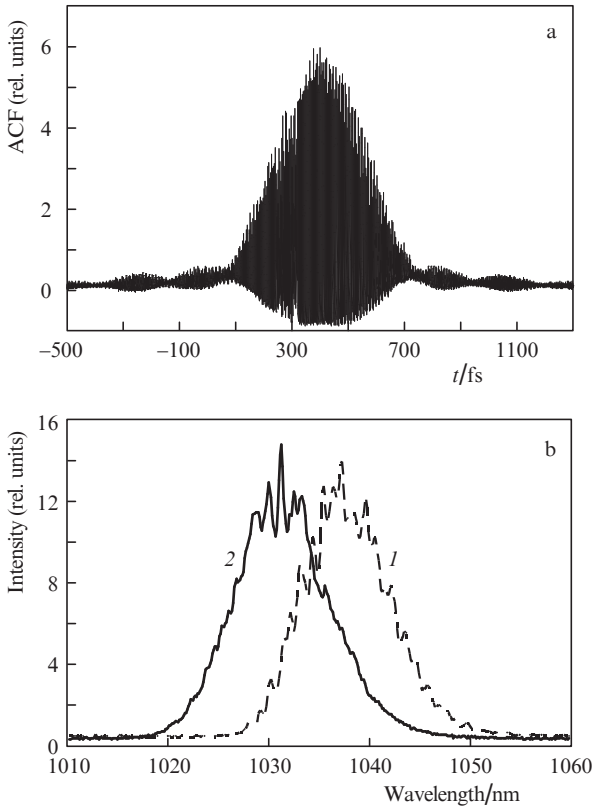

Figure 5. (a) ACF of the operating-channel pulse and (b) the spectra of radiation at the outputs of the (*1*) diagnostic and (*2*) operating channels of the fibre part of the cathode laser.

minimum duration. According to the measurement results, the pulse width does not exceed 235 fs for the diagnostic channel and 192 fs for the operating channel.

Figure 6 shows a CCF obtained with our cross-correlator. For the temporal intensity profile $I(t) = \cosh^{-2}(1.76t/\Delta t)$, the pulse width Δt can be estimated as 335 fs. Its difference from the pulse width derived from the ACF (235 fs) can be explained by rather large path lengths of the diagnostic and operating beams in air (more than 5 m) and in optical fibres (more than 80 m). Fluctuations of the difference in these lengths may be as high as 0.1 mm, which would lead to an increase in the minimum pulse width that can be measured by the cross-correlator to 335 fs.

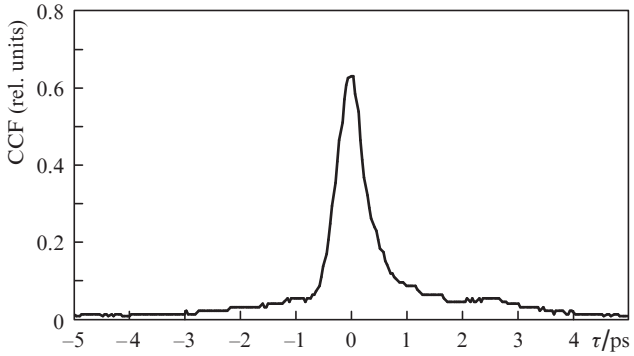

Figure 6. CCF of ultrashort radiation pulses in the operating and diagnostic channels.

As was mentioned above, a high scan rate is necessary for a laser operating in the regime of fairly long (300 μs) but rarely repeating (from 1 to 10 Hz) trains. The operating capacity of the cross-correlator was verified at scan rates from 4 to 1600 cm s^{-1}. To this end, we calibrated the device with the aid of an external micrometer air delay line. The calibration was performed by measuring the displacement of the correlogram profile caused by the introduction of a known additional delay into the diagnostic channel. Thus, one can obtain a calibration proportionality factor K between the pulse delay in the diagnostic channel and the voltage applied to the piezoceramic washer. To increase the calibration accuracy, the operating-channel pulse was compressed to the Fourier limit during calibration. Figure 7 shows the dependence of the calibration factor K on the scan rate V. As one would expect, the attainable amplitude of fibre extension is somewhat smaller at high scan rates; therefore, the calibration factor slightly decreases. This can easily be taken into account in the cross-correlator operation.

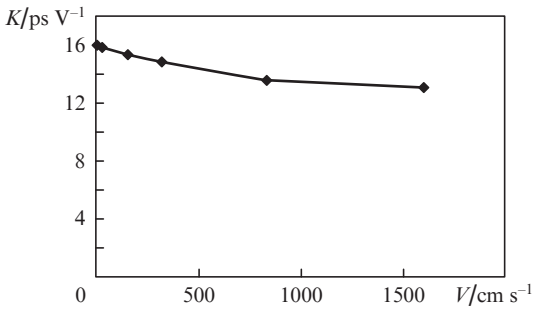

Figure 7. Dependence of the calibration factor K on the scan rate V.

Other important characteristics of the cross-correlator are the linearity of the fibre-scanner scan rate and the scan window. Although the temporal profile of the linearly increasing voltage applied to the electrodes of the scanner piezoceramic washer does not contain any sharp jumps, the nonzero spectral width of the control voltage is sufficient to excite mechanical resonances in the washer, which lead to a change in the spatial delay rate. These changes were also measured using an external air motorised delay line. Figure 8 shows the dependence of the scan rate V on the time delay of the diagnostic-

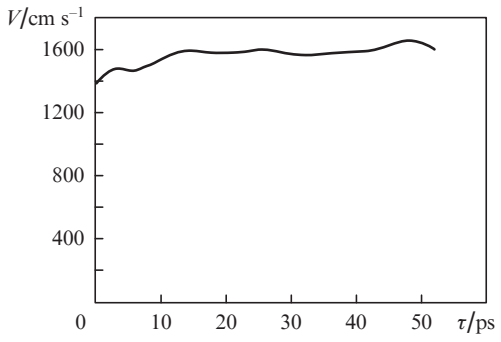

Figure 8. Dependence of the scan rate on the time delay of the diagnostic-channel pulse.

channel pulse at the maximum (available in our device) rate of increase in the voltage across the piezoceramic washer: 400 V ms^{-1}. It can be seen that, for a scan window width t_w = 52 ps, the relative change in the rate ($\Delta V/V$) does not exceed $\pm 8\%$, for t_w = 30 ps this change is $\pm 1.5\%$, and for t_w = 15 ps it is $\pm 0.5\%$.

The obtained limiting rate V (above 1600 cm s^{-1}) allows one to scan operating-channel pulses with widths up to 15 ps during a 300-μs macropulse. The limiting number of 'scans' that can be done using a diagnostic 200-fs pulse may reach 50. This number is quite sufficient for measuring the parameters of a 3D ellipsoidal 6-ps pulse.

Figure 1 shows that, if the pulse in the diagnostic channel is much shorter than the operating-channel pulse ($t_d \ll t_m$) and the transverse sizes of the beams, d_d and d_m, satisfy the relation $d_d \gg d_m$, one can measure transverse intensity distributions for the second-harmonic beam at different delays of diagnostic-channel pulses in order to reconstruct the spatial and 3D temporal structure of operating-channel pulses. In the experiments described here, we used Gaussian beams with a bell-shaped time profile. Different transverse intensity distributions for the operating-channel beam, obtained with a CCD camera, are similar to Gaussian but have different amplitudes. The shape of the dependences of the intensity distributions integrated over spatial coordinates on the time delay between the operating and diagnostic pulses reproduces the CCF profile. It can be seen in Fig. 9 that the CCF shape recorded with a photodiode reproduces with a high accuracy the CCF shape obtained by integrating the intensity distribution over the cross section.

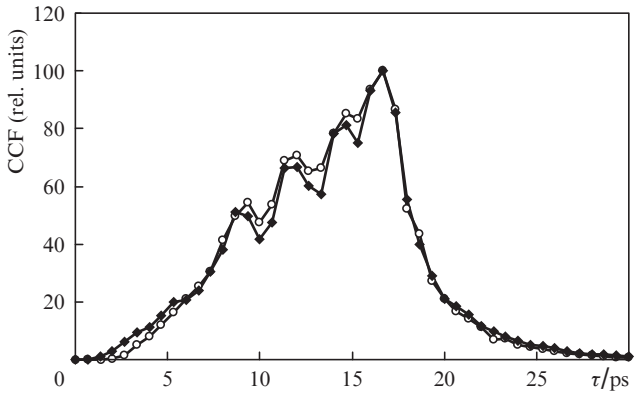

Figure 9. CCFs obtained (○) using a photodiode and (♦) by integrating the intensity distribution over the cross section of second-harmonic pulses, using a CCD camera.

6. Conclusions

We considered a scanning cross-correlator aimed at testing the spatial and temporal 3D structure of ellipsoidal pulses emitted by the cathode laser of the photo-injector of linear electron accelerator.

The above-described physical model of the cross-correlator and the numerical code formed on its basis made it possible to estimate the distortions of the spatial and temporal 3D structure of pulses at the experimentally attainable accuracy of adjusting the nonlinear crystal of the cross-correlator.

The regime of cathode-laser operation imposes stringent requirements on the rate of change in the pulse spatial delay in the correlator diagnostic channel. For example, to implement scanning of an operating-channel pulse with a width of 7 ps during 300 μs, the minimum rate of change in the delay of diagnostic-channel pulse should exceed 700 cm s^{-1}. The design of the delay line (based on a single-mode, polarisation-retaining optical fibre, wound as a spiral onto a piezoceramic washer) used in the cross-correlator under consideration, provided rates exceeding 1600 cm s^{-1}, which made it possible to scan operating-channel pulses with widths to 16 ps for a time of 300 μs.

The calibration of the correlator, performed at different extension rates of the optical fiber of the diagnostic-channel delay line, showed that the calibration factor at high rates decreases only slightly, and this decrease can always be taken into account in the correlator measurements.

The scan-window width in our design of the delay line exceeds 50 ps during a scan time of 1 ms, and the corresponding amplitude of the pulse spatial delay in the diagnostic channel is larger than 15 mm. Under these conditions, the relative change in the scan rate does not exceed 16%. For the scan window width corresponding to the operating-channel width of 6–7 ps, it is no more than 1%.

Preliminary experiments with the cross-correlator showed that its time resolution is 200–300 fs. The CCD camera, which cannot record more than 60 frames per second, allowed us to obtain images of transverse distributions of the cross-correlator pulse intensity at different time delays τ within the scan window. The CCD data are in good agreement with the CCF recorded using photodiodes.

Furthermore, we propose to use the above-described cross-correlator in the UV range (fourth harmonic of a Yb laser with λ = 250–260 nm). To this end, the nonlinear crystal in the cross-correlator will be replaced with a BBO crystal, cut so as to implement a nonlinear process with subtraction of the fundamental-harmonic frequency from the fourth-harmonic frequency in it. This scheme is in good agreement with the concept of a correlator operating at the fundamental lasing frequency, which was proposed in this study. The third-harmonic power generated in this process (at λ = 340 nm) can easily be measured by photodiodes, while the spatial intensity distribution can easily be visualised using a high-speed CCD camera. With allowance for the fact that the effective nonlinearity of BBO crystals during frequency doubling is close to that during third-harmonic generation, all our conclusions obviously hold true for the cross-correlator operation in the UV range.

Acknowledgements. This work was supported by the Russian Foundation for Basic Research (Grant No. 13-02-91323 sig_a) and the Ministry of Education and Science of the Russian Federation (State Contract No. 14.518.11.7071).

References

1. *Interim Report of the Scientific and Technical Issues (XFEL-STI) Working Group on a European XFEL Facility in Hamburg* (Hamburg, 2005).
2. Krasilnikov M., Stephan F., Asova G., Grabosch H.-J., Groß M., Hakobyan L., Isaev I., Ivanisenko Y., Jachmann L., Khojoyan M., Klemz G., Köhler W., Mahgoub M., Malyutin D., Nozdrin M., Oppelt A., Otevrel M., Petrosyan B., Rimjaem S., Shapovalov A., Vashchenko G., Weidinger S., Wenndorff R., Flöttmann K., Hoffmann M., Lederer S., Schlarb H., Schreiber S., Templin I.,

Will I., Paramonov V., Richter D. *Phys. Rev. Spec. Top. Accel. Beams*, **15**, 100701 (2012).
3. Tsuchiya K., Higashi Y., Hisamatsu H., Masuzawa M., Matsumoto H., Mitsuda C., Noguchi S., Ohuchi N., Okamura T., Saito K., Terashima A., Toge N., Hayano H. *Proc. EPAC' 2006* (Edinburg, Scotland, 2006) pp 505–507.
4. Csatari D.M. et al. *Nucl. Instrum. Methods Phys. Res., Sect. A*, **659**, 1 (2011).
5. Kapchinskij I.M., Vladimirskij V.V. *Proc. 2-nd Conf. on High Energy Accelerators and Instrumentation (CERN)* (Geneva, 1959) pp 274–288.
6. Will I., Klemz G. *Opt. Express*, **16** (18), 14922 (2008).
7. Gelikonov V.M., Gelikonov G.V., Ksenofontov S.Yu., Terpelov D.A., Shilyagin P.A. *Instr. Exp. Tech.*, **53** (3), 443 (2010).
8. www.photron.com.
9. Ippen E.P., Shank C.V., in *Ultrashort Light Pulses, Picosecond Techniques and Applications* (Berlin–Hidelberg–New York: Springer-Verlag, 1977) pp 90–92.